

**Topographic Change Detection using Pre- and Post-Flood LiDAR Data from Boulder, Colorado**

Term Project

GEOG 603: Remote Sensing Basics and Beyond

Maja Kucharczyk

April 11, 2016

## **Abstract**

A major flood occurred in Boulder, Colorado in September 2013. Light detection and ranging (LiDAR) data, obtained two months before and one month after the flood, was converted into pre- and post-flood digital terrain models (DTMs), which were differenced into a DTM of a difference (DOD). The DOD was used to calculate stream channel erosion and deposition volume. The post-flood DTM was used to calculate the slope aspect of possible debris flows. The noise and limitations of the data were examined.

## **1. Introduction**

### **1.1 Background**

Floods are catastrophic events that can result in human fatalities and billions of dollars in damage. Between September 9 and 16, 2013, Boulder, Colorado experienced heavy and persistent rainfall exceeding 450 millimeters that resulted in flash floods, landslides, and debris flows (Gochis et al., 2015). The flood was a 1,000-year precipitation event (Goulden & Kampe, 2014). As a result, eight people died and infrastructure damage exceeded two billion dollars (Gochis et al., 2015).

### **1.2 Past Studies**

According to Coe et al. (2014), over 1,138 debris flows occurred in the greater Boulder region as a result of the flood. The debris flows occurred when heavy rainfall liquefied and rapidly moved masses of soil downslope. Out of the 1,138 debris flows Coe et al. (2014) measured in the field and later digitized using satellite imagery, 78 percent (%) initiated on south-facing slopes. The authors believe one contributing factor to the trend could be that south-facing slopes lack thick tree cover and contain abundant rock outcrops. The geospatial data for the 1,138 debris flows observed in the field by Coe et al. (2014) could not be located. Luckily, the Colorado Geological Survey produced a geospatial dataset

of debris flow locations shortly after the flood in December, 2013 (Morgan, Fitzgerald, & Morgan, 2013).

This geospatial dataset was also digitized using pre- and post-flood satellite imagery.

Conveniently, the National Ecological Observatory Network (NEON) of Boulder, Colorado, collected airborne light detection and ranging (LiDAR) data over Boulder approximately two months before the flood occurred and one month after the flood (Goulden & Kampe, 2014). The timing of the data collection introduces an opportunity for temporal analysis of topographic change due to the flood. Specifically, the pre- and post-flood LiDAR datasets can be differenced in order to locate evidence of flood-induced sediment transport in the form of stream channel erosion and deposition. The slope aspect of debris flow locations can also be analyzed.

### **1.3 Objectives**

For this term project, there are three main objectives:

- 1) Use the pre- and post-flood LiDAR data to produce pre- and post-flood digital terrain models (DTMs), followed by a DTM of difference (DOD)
- 2) Use the DOD to locate areas of sediment erosion and deposition along a stream channel and calculate erosion and deposition volume
- 3) Use the post-flood DTM to determine the slope aspects of the satellite imagery-derived debris flow locations by Morgan, Fitzgerald, & Morgan (2014) and compare the results to those obtained by Coe et al. (2014)

## **2. Methodology**

### **2.1 Study Area**

Figure 1 shows the approximate location of Boulder, Colorado, United States. Boulder is situated in the foothills and plains east of the Rocky Mountains, approximately 45 kilometers northwest of Denver. Similar to Calgary, Boulder is susceptible to flooding due to its proximity to the Rocky Mountains.

### **2.2 Data**

#### **2.2.1 LiDAR Data Overview**

NEON collected piloted airborne LiDAR data on June 26 and 27, 2013, approximately two months prior to the flood, and again on October 8, 2013, approximately one month after the flood (NEON, 2016). The boundaries of the pre- and post-flood flights are shown in Figure 2. Table 1 summarizes the characteristics of the pre- and post-flood LiDAR datasets. The two datasets obtained a similar footprint using the same aircraft, LiDAR sensor, and similar flight altitudes. The datasets resulted in similar total point counts, average point density, and average point spacing.

Table 1. NEON LiDAR data acquisition parameters. Modified from (Goulden & Kampe, 2014).

<b>Parameter</b>	<b><u>Pre-flood survey</u></b>	<b><u>Post-flood survey</u></b>
<b>Date</b>	June 26-27, 2013	October 8, 2013
<b>Aircraft</b>	Twin Otter	Twin Otter
<b>LiDAR sensor</b>	Optech Gemini (serial #11SEN287)	Optech Gemini (serial #11SEN287)
<b>Mean flight altitude</b>	1500 meters above ground level	1800 meters above ground level
<b>Pulse repetition frequency</b>	70 kHz	70 kHz
<b>Scan frequency</b>	33 Hz	33 Hz
<b>Beam divergence (1/e)</b>	0.8 mRad	0.8 mRad
<b>Half scan angle</b>	18°	18°
<b>Point observations acquired</b>	703,000,000+	729,000,000+
<b>Avg. point density</b>	3.0 pts/m <sup>2</sup>	2.88 pts/m <sup>2</sup>
<b>Avg. point spacing</b>	0.58 m	0.59 m

# Figure 1. General Location of Boulder, Colorado, USA

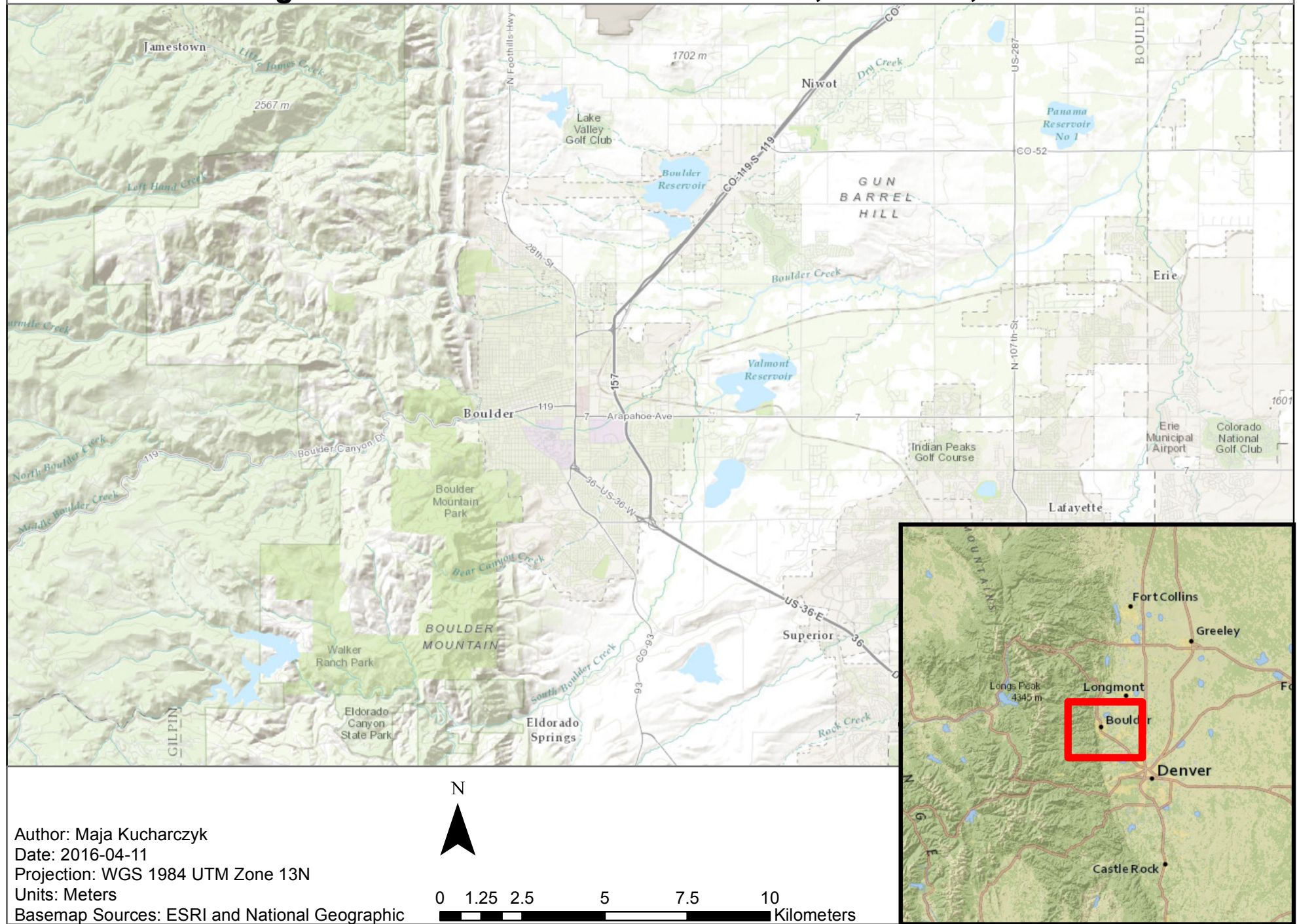
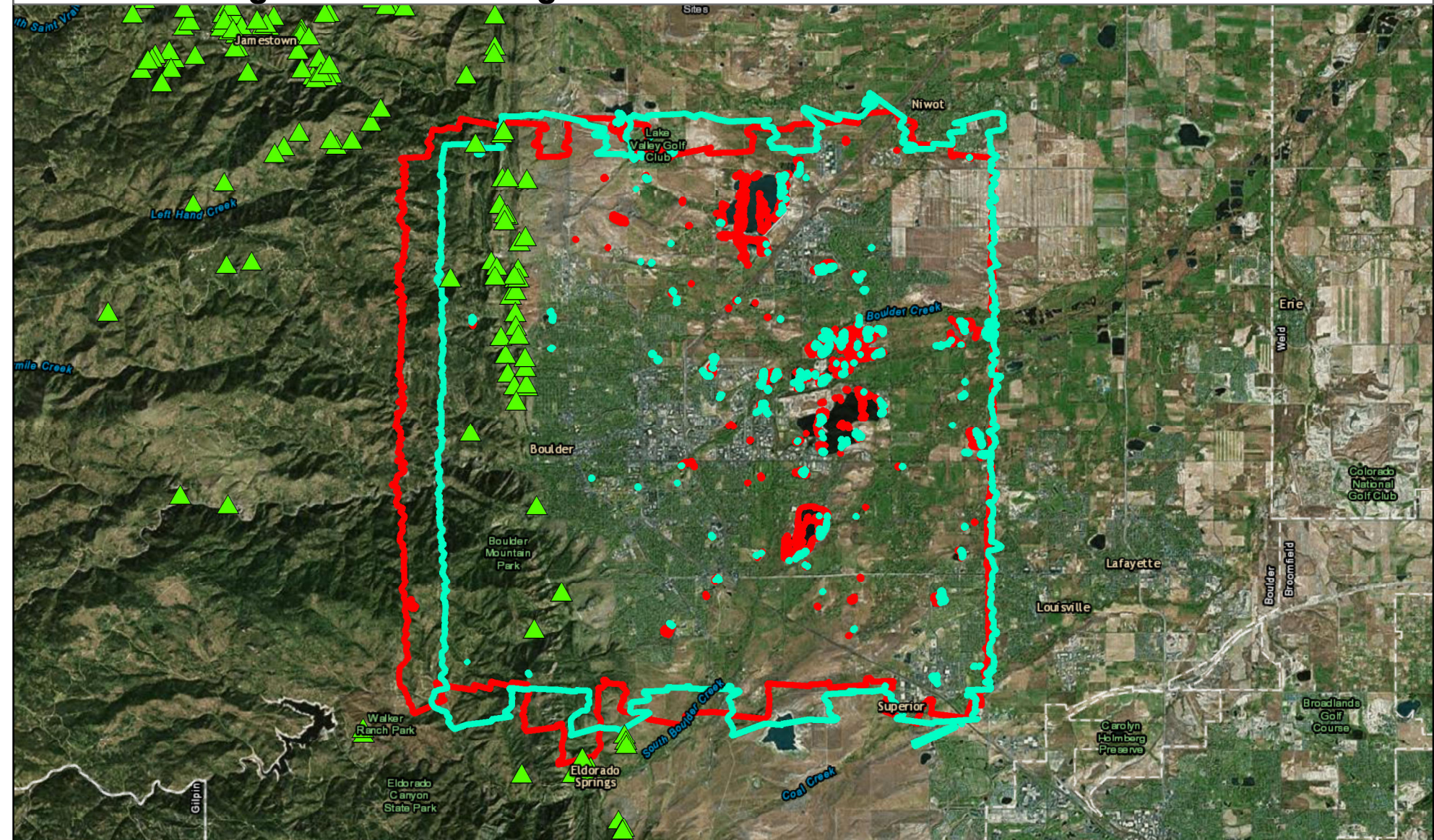


## Figure 2. LiDAR Flight Boundaries and Possible Debris Flows



Author: Maja Kucharczyk

Date: 2016-04-11

Projection: WGS 1984 UTM Zone 13N

Units: Meters

Basemap Sources: ESRI

Flight Boundaries: NEON (2016)

Debris Flows: Morgan, Fitzgerald, & Morgan (2014)

### Legend

Pre-flood LiDAR Flight Boundary

Post-flood LiDAR Flight Boundary

Possible Debris Flow Location

0 1.25 2.5 5 7.5 10 Kilometers

Since NEON is a publicly funded scientific research organization, the airborne data is available to the public and was obtained by request through NEON (2016). The data was delivered to the user in the form of a classified point cloud; points were classified as either ground, building, vegetation, or unclassified (NEON, 2016).

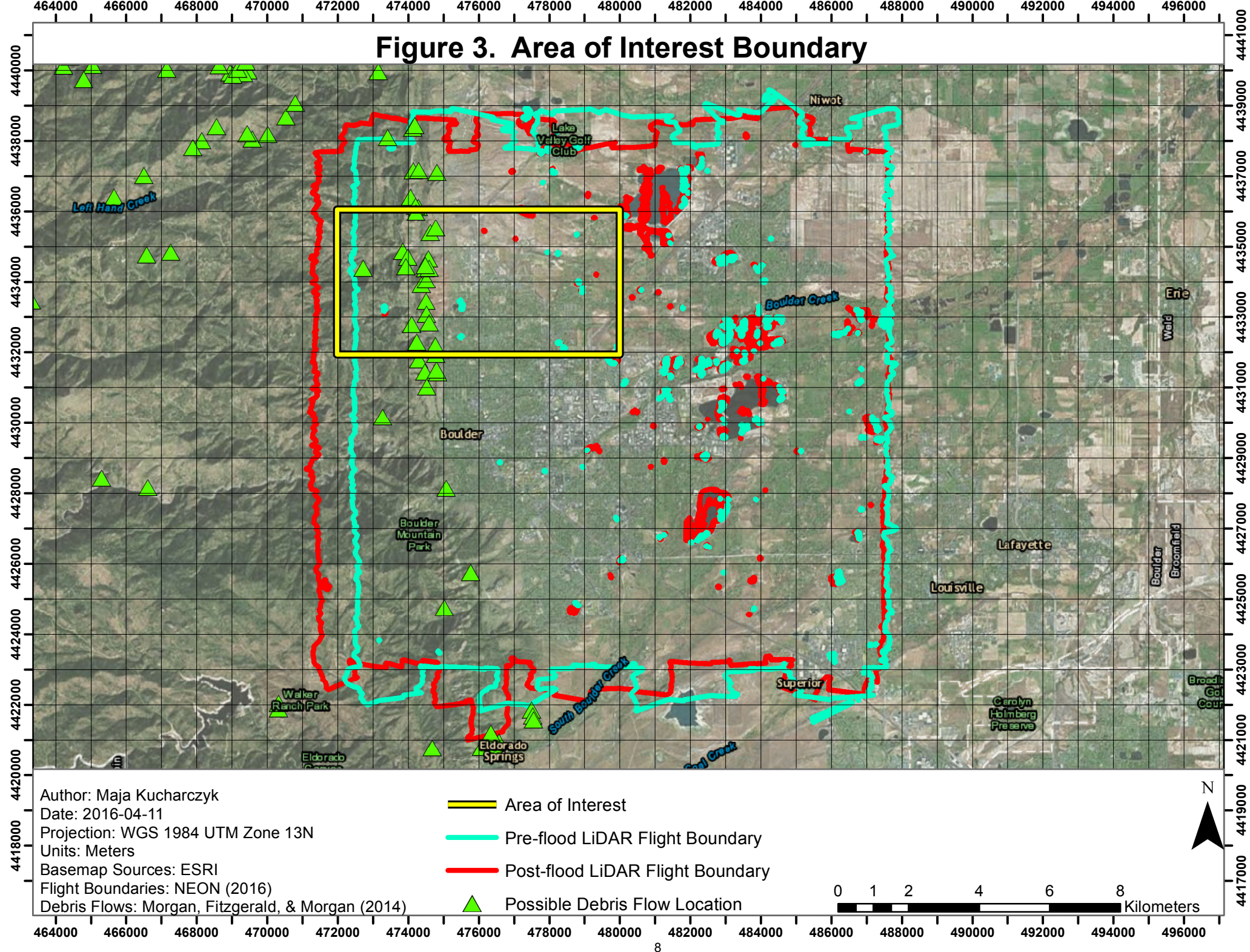
### **2.2.2 Debris Flow Locations**

The Colorado Geological Survey used pre- and post-flood satellite imagery with spatial resolutions of 2.5-5 meters (SPOT 5), 0.46 meters (Digital Globe Worldview-2), and 1 meter (USDA NAIP) to identify possible debris flow locations. The authors produced a point shapefile of the locations, as shown in Figure 1. This shapefile was acquired by download through Morgan, Fitzgerald, & Morgan (2014).

### **2.2.3 Area of Interest Selection**

Due to the file size of the LiDAR datasets (over 700 million data points each), an area of interest (AOI) was delineated based on potential debris flow abundance and stream channel presence. The AOI is shown in Figure 3. The LiDAR datasets are composed of one-square-kilometer ( $1 \text{ km}^2$ ) tiles whose boundaries are defined by the WGS 1984 UTM Zone 13N coordinate system grid. The AOI includes 32 tiles, or  $32 \text{ km}^2$  of area.

### Figure 3. Area of Interest Boundary



**2.3 Objective 1:** Use the LiDAR data to produce pre- and post-flood digital terrain models (DTMs), followed by a DTM of difference (DOD)

### **2.3.1 LiDAR Point Cloud Processing**

#### **2.3.1.1 Extraction of Compressed Files**

The pre- and post-flood LiDAR datasets were delivered to the user in 1-km<sup>2</sup> tiles in a compressed format, “.laz” or “LAZ”. The LAZ files were be extracted by an ESRI ArcGIS Extension tool, LAStools, which was downloaded from RapidLasso (2016). The 32 files from each dataset were input into the “laszip” tool of the extension, and were extracted to uncompressed LAS 1.3 files. LAS 1.3 is the standard LiDAR data format as defined by the American Society for Photogrammetry and Remote Sensing (ASPRS, 2010).

#### **2.3.1.2 Creating LAS Datasets**

Using ArcCatalog (ArcGIS 10.3), a project geodatabase was created (**Boulder\_2013\_Flood\_LiDAR.gdb**). With 32 LAS tiles for each dataset (pre- and post-flood), a LAS Dataset was created for each dataset to help organize the files. In ArcCatalog, a LAS Dataset was created for the pre-flood data using the Create LAS Dataset tool. The input files consisted of all of the pre-flood LAS files. The output LAS dataset was specified (**preflood\_las\_dataset.lasd**). By viewing the LAS dataset properties, the user was able to determine the range of average point spacing of all 32 LAS files (0.5-0.7m). The process was repeated for the post-flood LAS files. The output was specified (**postflood\_las\_dataset.lasd**), and the range of average point spacing was obtained (0.5-0.6m).

#### **2.3.1.3 Creating Mosaic Datasets and Exporting DTMs**

In order to export the point clouds of each LAS Dataset to a DTM, a Mosaic Dataset had to be created for each LAS Dataset. Using ArcCatalog, a new pre-flood Mosaic Dataset

(**Preflood\_LAS\_Mosaic**) was added to the project geodatabase. The projected coordinate system was set to match the LAS files (WGS 1984 UTM Zone 13N). The Add Rasters To Mosaic Dataset tool was used to add the LAS Dataset to the Mosaic Dataset. Under “Raster Type”, “LAS Dataset” was specified. The pre-flood LAS Dataset (**preflood\_las\_dataset.lasd**) was added as an input. A screen capture of the dialog box is available in Appendix A (Figure A.1).

A yellow warning icon then appeared next to “Raster Type”, signifying that the “Raster Type Properties” dialog had to be opened and parameters had to be specified. The “Raster Type Properties” icon (second button to the right of “Raster Type”) was selected. To ensure that only points classified as “ground” would be included in the DTM, the user specified “ground” for “Class Types”. The output pixel size was specified as 1 meter, because the LAS datasets had a maximum average point spacing less than 1 meter. The “Cell Aggregation Type” was specified as “mean”, meaning that if multiple points were in one pixel, then the elevation value of the pixel would equal the mean elevation of the points within. “Void Filling” was set to “Linear (Triangulation)”, meaning that if a pixel did not contain any points, then the void area would be triangulated and linear interpolation would be used to estimate an elevation value for that pixel. A screen capture of the dialog box is included in Appendix A (Figure A.2).

The same process was repeated for the post-flood dataset. A new Mosaic Dataset (**Postflood\_LAS\_Mosaic**) was added to the project geodatabase, and the post-flood LAS Dataset (**postflood\_las\_dataset.lasd**) was added as an input. To obtain the final pre- and post-flood DTMs, both Mosaic Datasets were exported as Raster Datasets (**Preflood\_DTM**, **Postflood\_DTM**) to the geodatabase with a Pixel Type of 32-Bit Float.

### 2.3.2 Creating a DOD

Using ArcCatalog, the Minus tool was used to difference the two DTMs to create a DOD. The post-flood DTM was used as the DTM to subtract values from in order for positive DOD values to

represent areas of positive change (sediment deposition), and negative DOD values to represent areas of negative change (sediment erosion). The output raster dataset was specified (**Flood\_DOD**). A screen capture of the dialog box is available in Appendix A (Figure A.3).

The DOD contained noise along its western boundary. To remove the noise, the Raster Clip tool was used to clip the DOD at 472,750m on the western boundary. The output raster dataset was specified (**Flood\_DOD\_Clip**). To obtain statistics of the clipped DOD, the DOD was exported to a TIFF file (**DOD\_for\_Hist.tif**) and opened in PCI Geomatica Focus. Statistics and histograms were produced of the clipped DOD.

**2.4 Objective 2:** Use the DOD to locate areas of sediment erosion and deposition along a stream channel and calculate erosion and deposition volume

#### **2.4.1 Symbolize the DOD**

Using ArcMap, the DOD was symbolized with a two-ended color gradient, showing areas of negative change (erosion) as red and areas of positive change (deposition) as blue. The DOD was used to identify areas along a stream channel that have experienced relatively high amounts of erosion and deposition.

#### **2.4.2 Select Areas of Erosion and Deposition**

Two parts along a stream channel (one showing major erosion, and one showing major deposition) were chosen. A polygon feature class was digitized around the area of erosion (**Vol\_Poly\_1**) and the area of deposition (**Vol\_Poly\_2**). Using the Raster Clip tool, the pre- and post-flood DTMs were clipped using the two polygon feature classes representing major erosion and deposition along the

stream channel. Four output raster datasets were produced (**Preflood\_DTM\_Erosion**, **Postflood\_DTM\_Erosion**, **Preflood\_DTM\_Deposition**, **Postflood\_DTM\_Deposition**).

#### **2.4.3 Calculate Erosion and Deposition Volume Along a Stream Channel**

Using the Cut Fill tool in ArcMap, the erosion-area pre- and post-flood DTMs were input. Volumetric change was calculated for each pixel of the output raster dataset (**Erosion\_Volume**). Then, the deposition-area pre- and post-flood DTMs were input. Volumetric change was calculated for each pixel of the output raster dataset (**Deposition\_Volume**).

**2.5 Objective 3:** Use the post-flood DTM to determine the slope aspects of the satellite imagery-derived debris flows locations by Morgan, Fitzgerald, & Morgan (2014) and compare the results to those obtained by Coe et al. (2014)

##### **2.5.1 Calculate the Aspect of the Post-flood DTM**

The debris flow feature class (**Debris\_Flows**) from Morgan, Fitzgerald, & Morgan (2014) was mapped on top of the post-flood DTM. The post-flood DTM was used as opposed to the pre-flood DTM, because it is more representative of the topography at the time the debris flows existed. Nineteen out of 330 total debris flows were within the post-flood DTM boundaries.

In ArcMap, the Aspect tool was used to calculate the aspect of every pixel in the post-flood DTM. The post-flood DTM raster dataset was input into the Aspect tool, and the output raster dataset was specified (**Postflood\_Aspect**).

### **2.5.2 Extract the Aspects at the Debris Flow Locations**

In ArcMap, the Extract Values to Points tool was used to extract the aspect at each of the nineteen debris flow locations. The debris flow locations were the input point features, and the aspect raster dataset was the input raster. The output feature class was specified (**Debris\_Flows\_Aspects**). The aspect describes the downslope direction of the maximum rate of change (i.e. the direction of the steepest slope). A value of 0 degrees would be due north, a value of 90 degrees would be due east, a value of 180 degrees would be due south, and a value of 270 degrees would be due west. A value of -1 indicates a flat area with no downslope direction (ESRI, 2016).

### **3. Results and Discussion**

**3.1 Objective 1:** Use the LiDAR data to produce pre- and post-flood digital terrain models (DTMs), followed by a DTM of difference (DOD)

#### **3.1.1 DTMs**

The 1-meter spatial resolution pre- and post-flood DTMs are shown in Figures 4 and 5, respectively. The lowest elevation of the pre-flood DTM (1579.17m) corresponds well with that of the post-flood DTM (1579.44m). The highest elevation of the pre-flood DTM (2126.78m) is lower than that of the post-flood DTM (2135.29m), which can be attributed to the post-flood DTM extending further west and covering more mountainous terrain than the pre-flood DTM.

#### **3.1.2 DOD**

The DOD is shown in Figure 6. The maximum positive elevation change (89.73m) and the maximum negative elevation change (-71.99m) are unrealistic values and appear to be noise. The two-color gradient of blue for positive values and red for negative values shows red and blue noise along the western boundary of the DOD. A preliminary inspection of this noise would suggest that one of the DTMs did not cover that area, and therefore, the large voids were filled via interpolation. However, interpolation would not result in these large values, and both datasets covered the areas of noise.

To remove the noise, the DOD was clipped along its western boundary (Figure 7). The resulting maximum positive elevation change (16.09m) and maximum negative elevation change (-13.9m) were more realistic values than those of the original DOD. However, noise remained in the clipped DOD. Particularly, the urban area in the center of the clipped DOD had many high negative and positive values. Zooming into an urban area, the user was able to see evidence of point classification errors (Figure 8). Points on and around buildings were inconsistently classified between the pre- and post-flood LiDAR datasets, resulting in large elevation differences in urban areas.

**Figure 4. Pre-flood DTM**

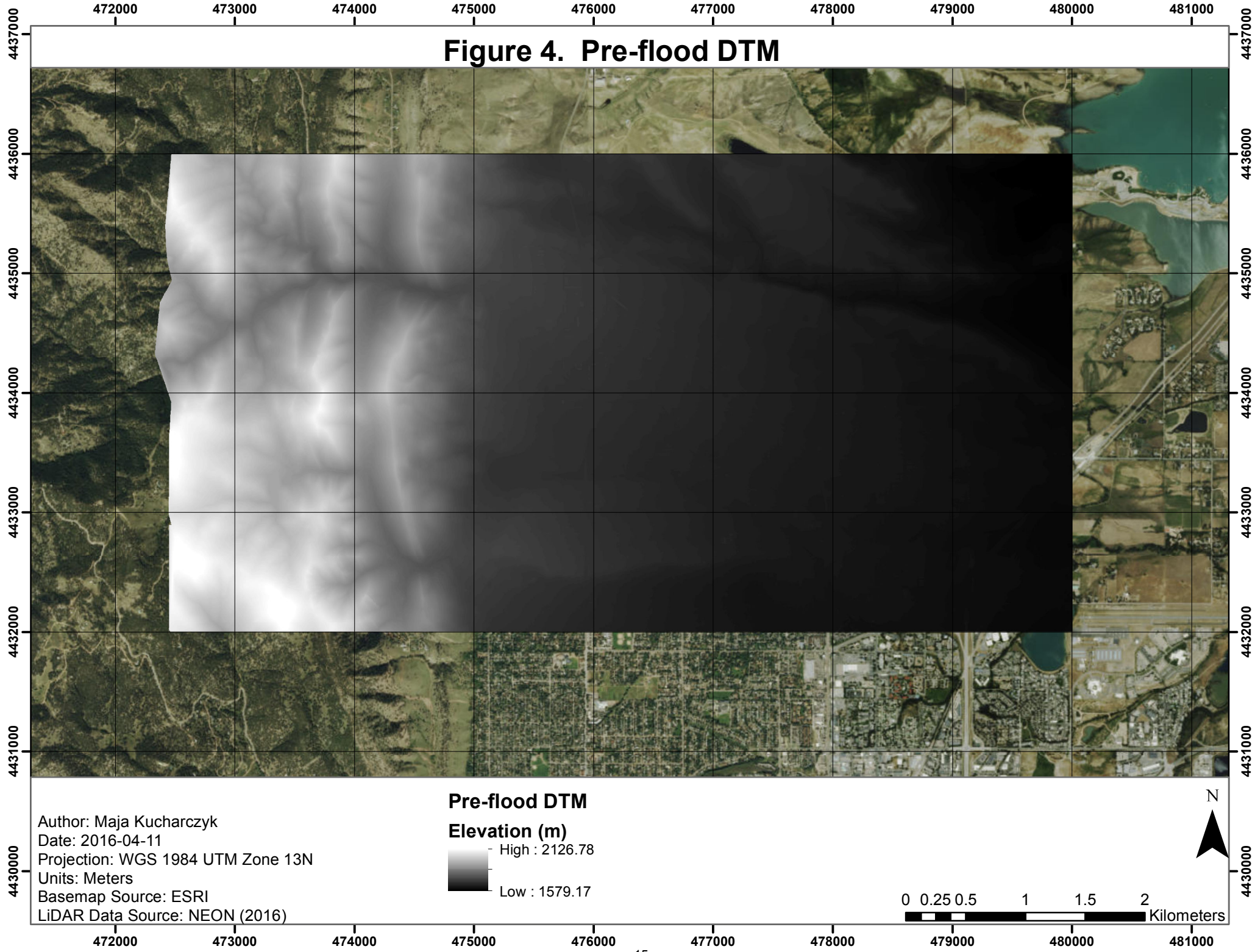


## Figure 5. Post-flood DTM

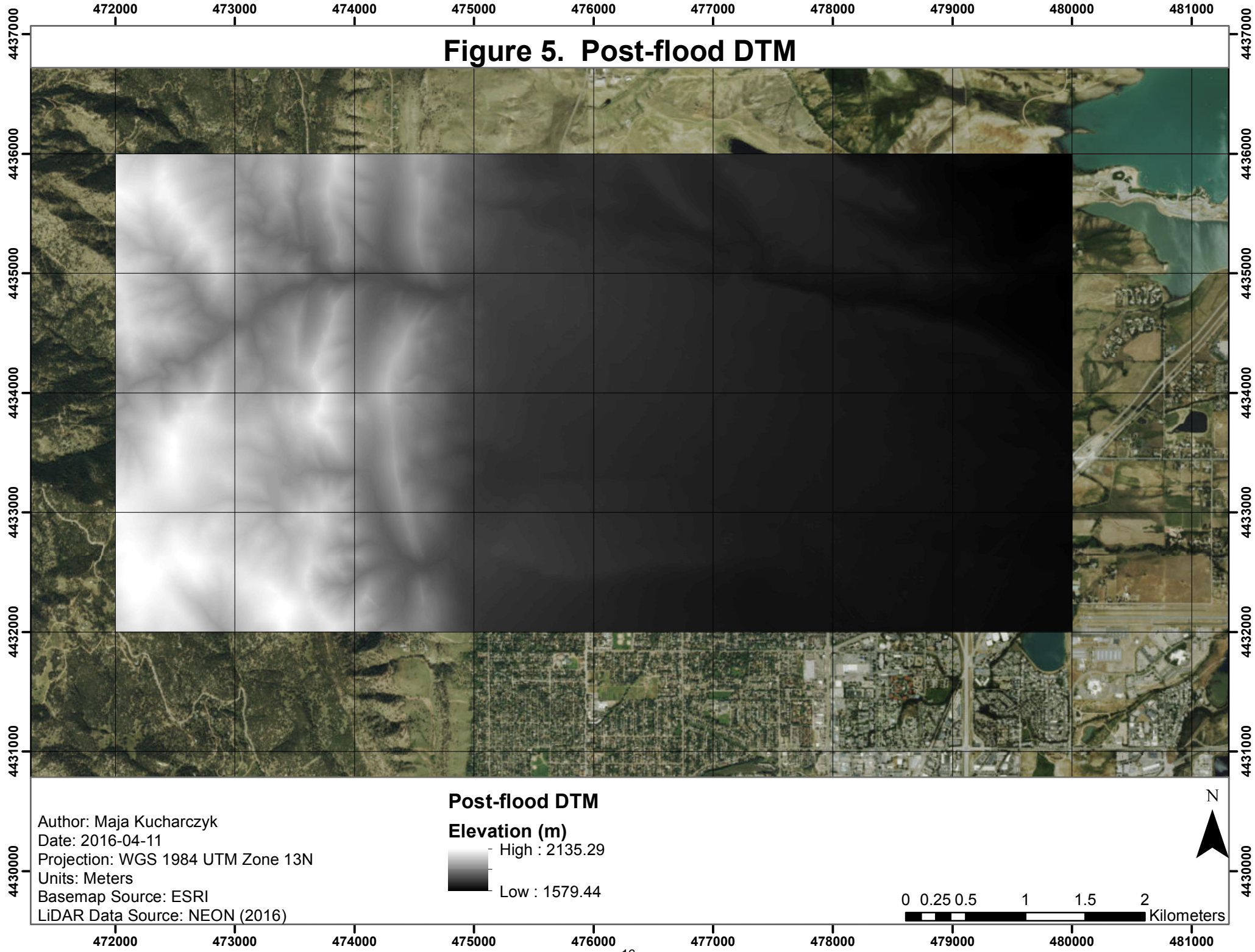


## Figure 6. DOD

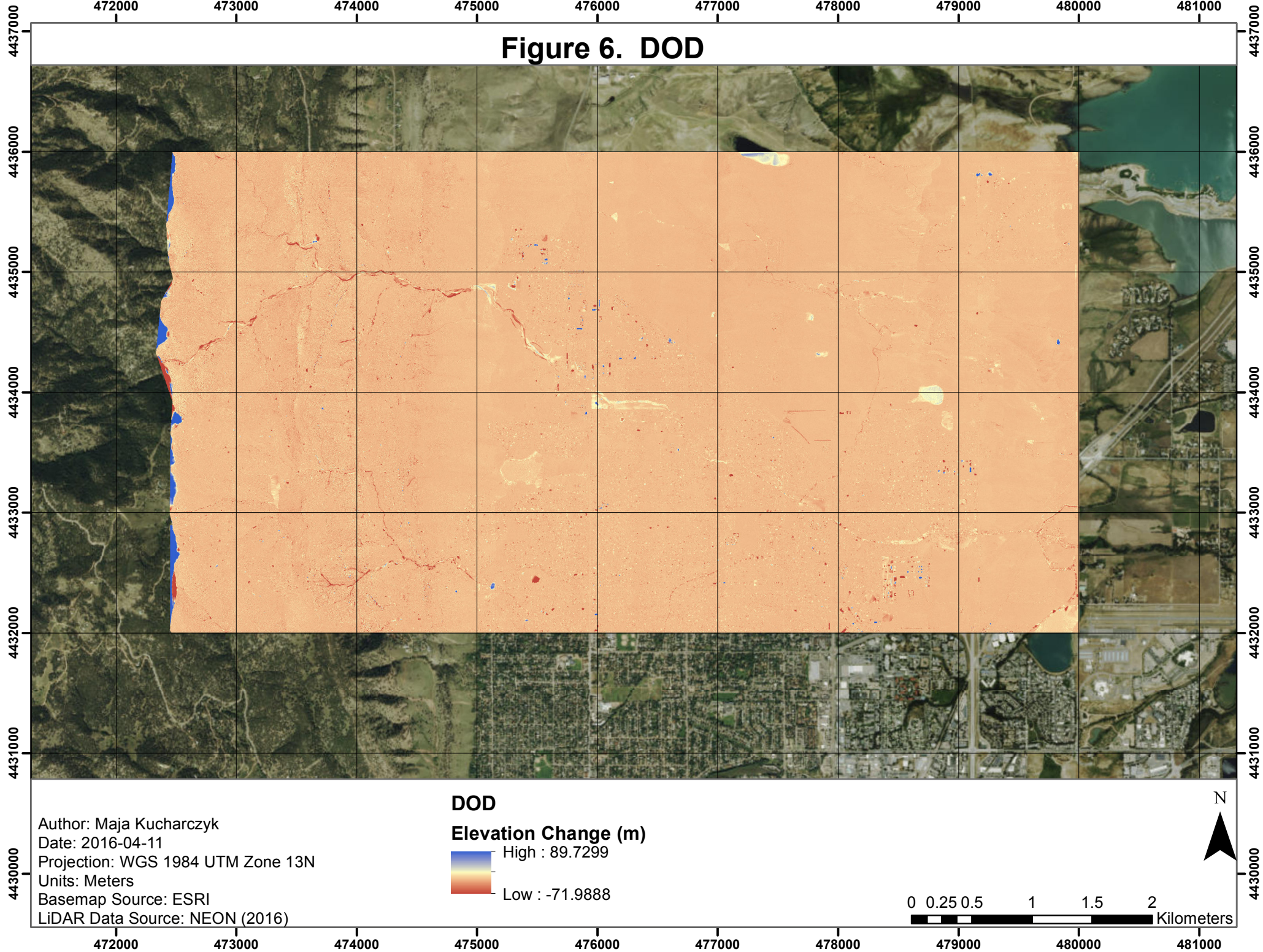
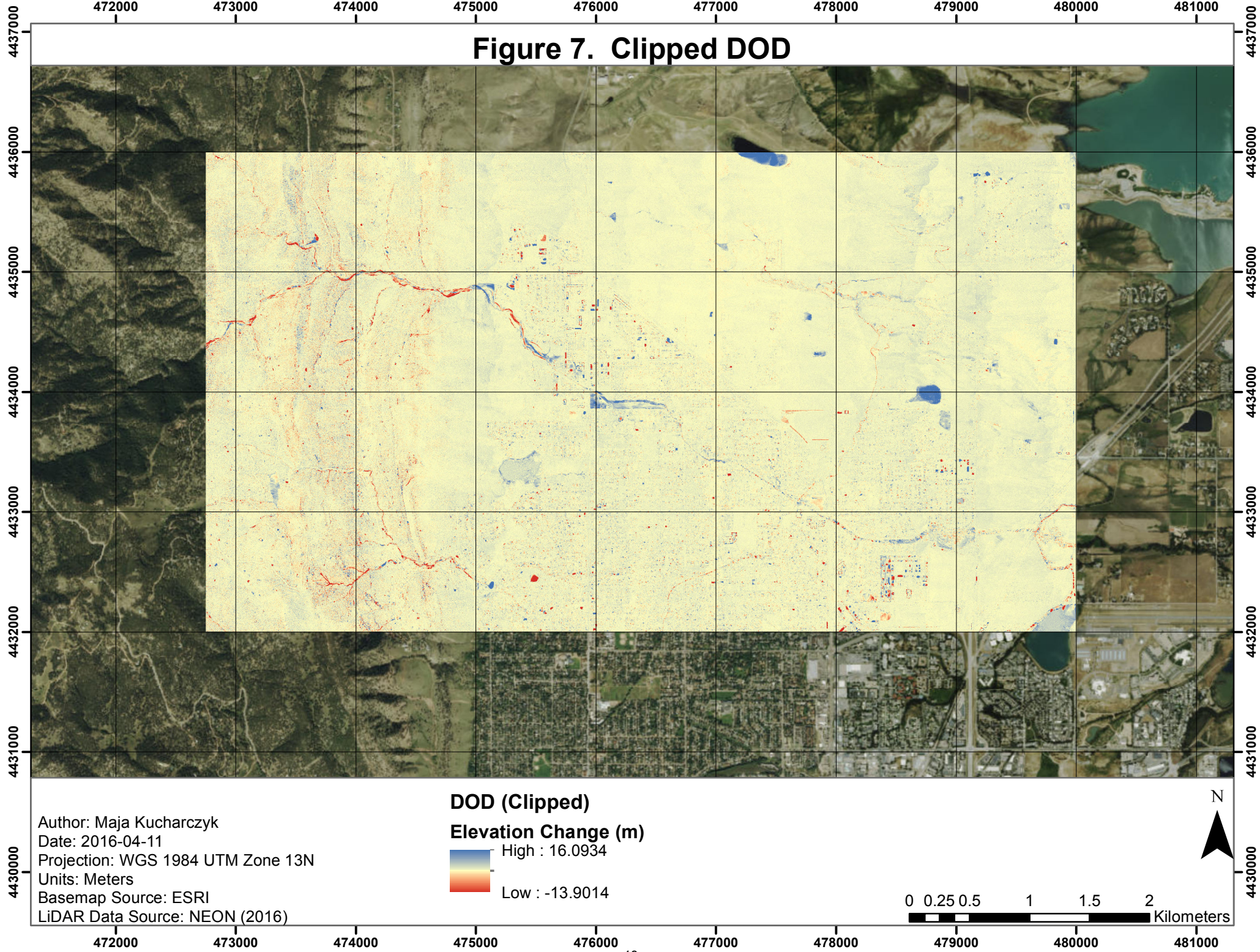


## Figure 7. Clipped DOD

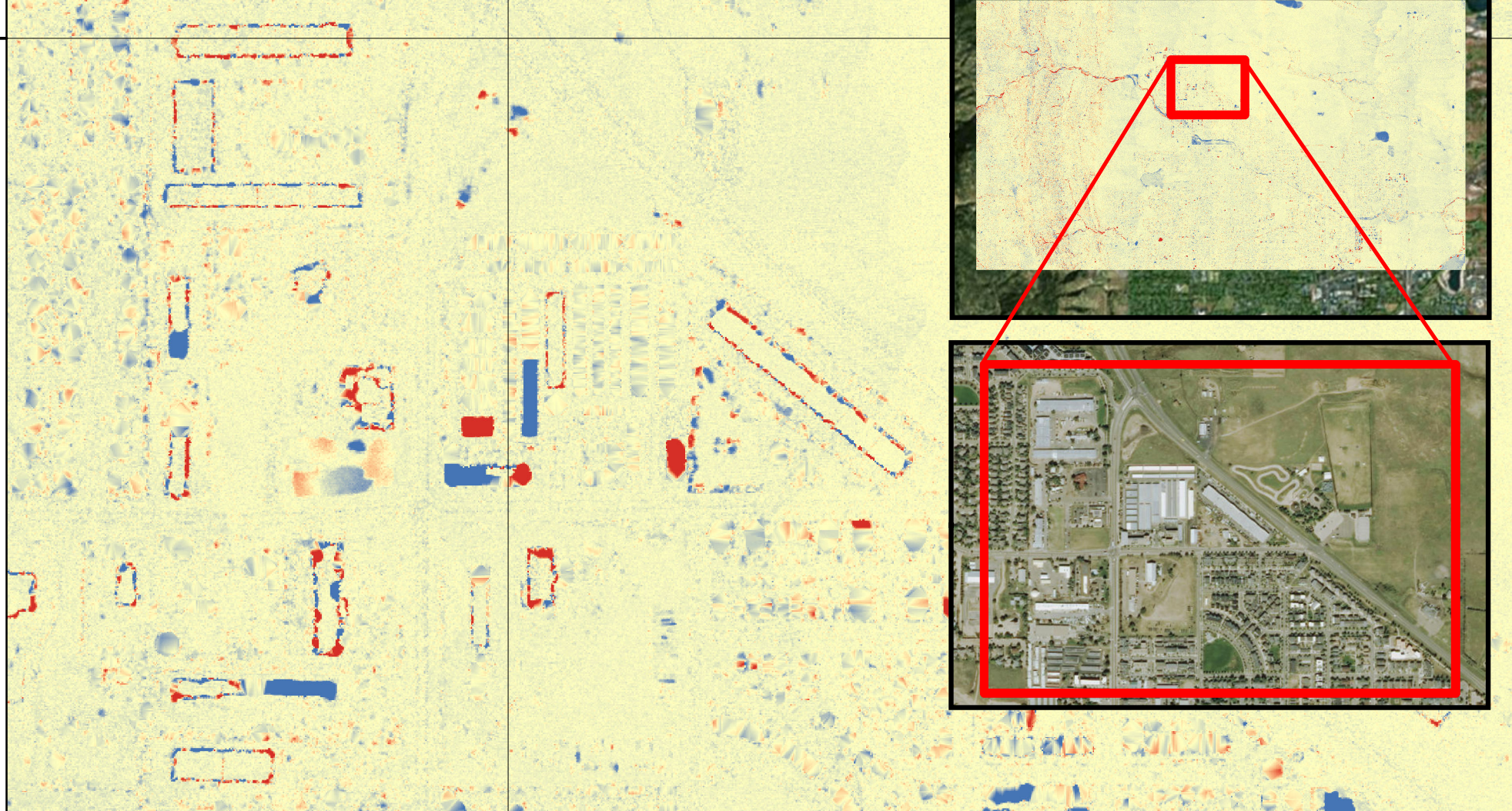


476000

## Figure 8. Urban Noise

4435000

4435000



Author: Maja Kucharczyk

Date: 2016-04-11

Projection: WGS 1984 UTM Zone 13N

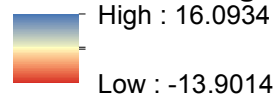
Units: Meters

Basemap Source: ESRI

LiDAR Data Source: NEON (2016)

### DOD (Clipped)

#### Elevation Change (m)



N



476000

To investigate the noise in the clipped DOD, summary statistics were calculated using PCI Geomatica Focus (Table 2). A histogram of the entire clipped DOD is shown in Figure 9. The data appears to be normally distributed. A standard deviation of 0.26123m of normally distributed data indicates that approximately 68% of the values (elevation change) are within 0.13m (half the standard deviation) from either side of the mean. Furthermore, 95% of the values (elevation change) are within 0.26m (one standard deviation) from either side of the mean. Finally, 99.7% of the values (elevation change) are within 0.39m (1.5 standard deviations) from either side of the mean. These percentages would be accurate for a perfect normal distribution; however, since the clipped DOD has an approximate normal distribution, it can be assumed that 99% of the values (elevation change) are between -1m and +1m. Therefore, any values outside of this range can be discarded as noise. The histogram of clipped DOD values ranging from -1 to 1 are shown in Figure 10.

Table 2. Summary statistics of the clipped DOD. Modified from PCI Geomatica Focus.

<b>Total number of pixels</b>	28,999,996
<b>Minimum Value</b>	-13.9014
<b>Maximum Value</b>	16.0934
<b>Mean Value</b>	0.0158945
<b>Mode Value</b>	0
<b>Median Value</b>	0.0198992
<b>Standard Deviation</b>	0.26123

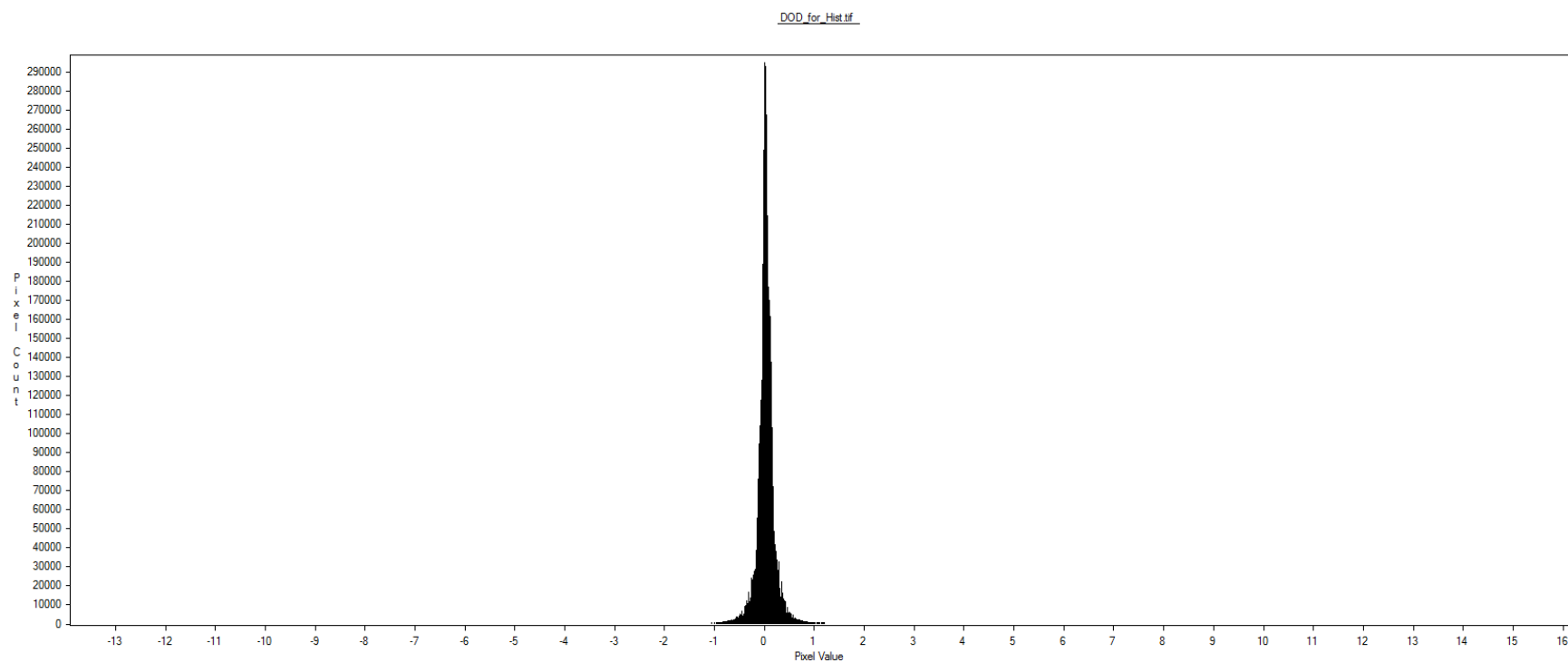


Figure 9. Histogram of the clipped DOD, representing the entire range of values (-13.9014-16.0934m). Copied from PCI Geomatica Focus.

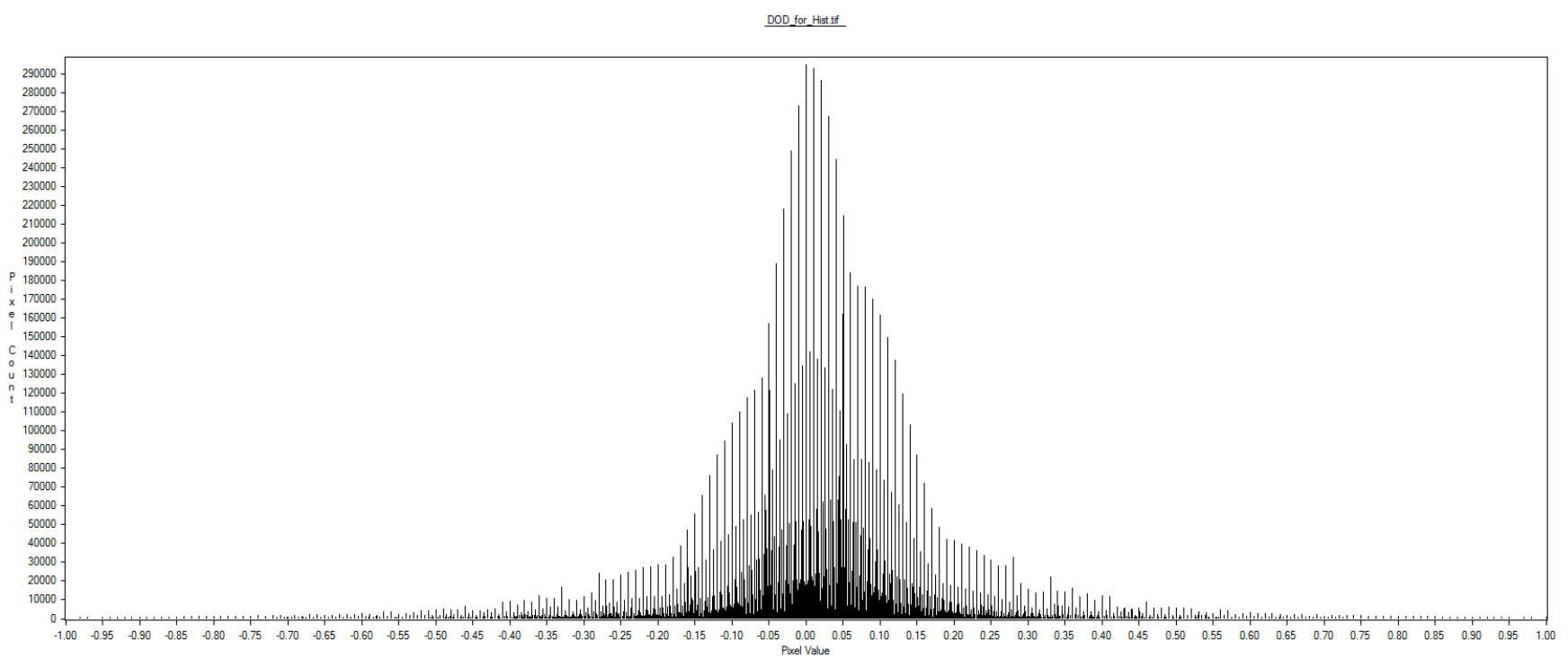


Figure 10. Histogram of the clipped DOD, with a smaller range of values (-1 to 1m). Copied from PCI Geomatica Focus.

A newly symbolized DOD, showing a range of values from -1m to 1m, is shown in Figure 11.

With a smaller range of displayed elevation change values, fluvial elevation changes are highlighted with deeper blue and red colors. Stream channels are apparent in the northwest portion of the DOD.

**3.2 Objective 2:** Use the DOD to locate areas of sediment erosion and deposition along a stream channel and calculate erosion and deposition volume

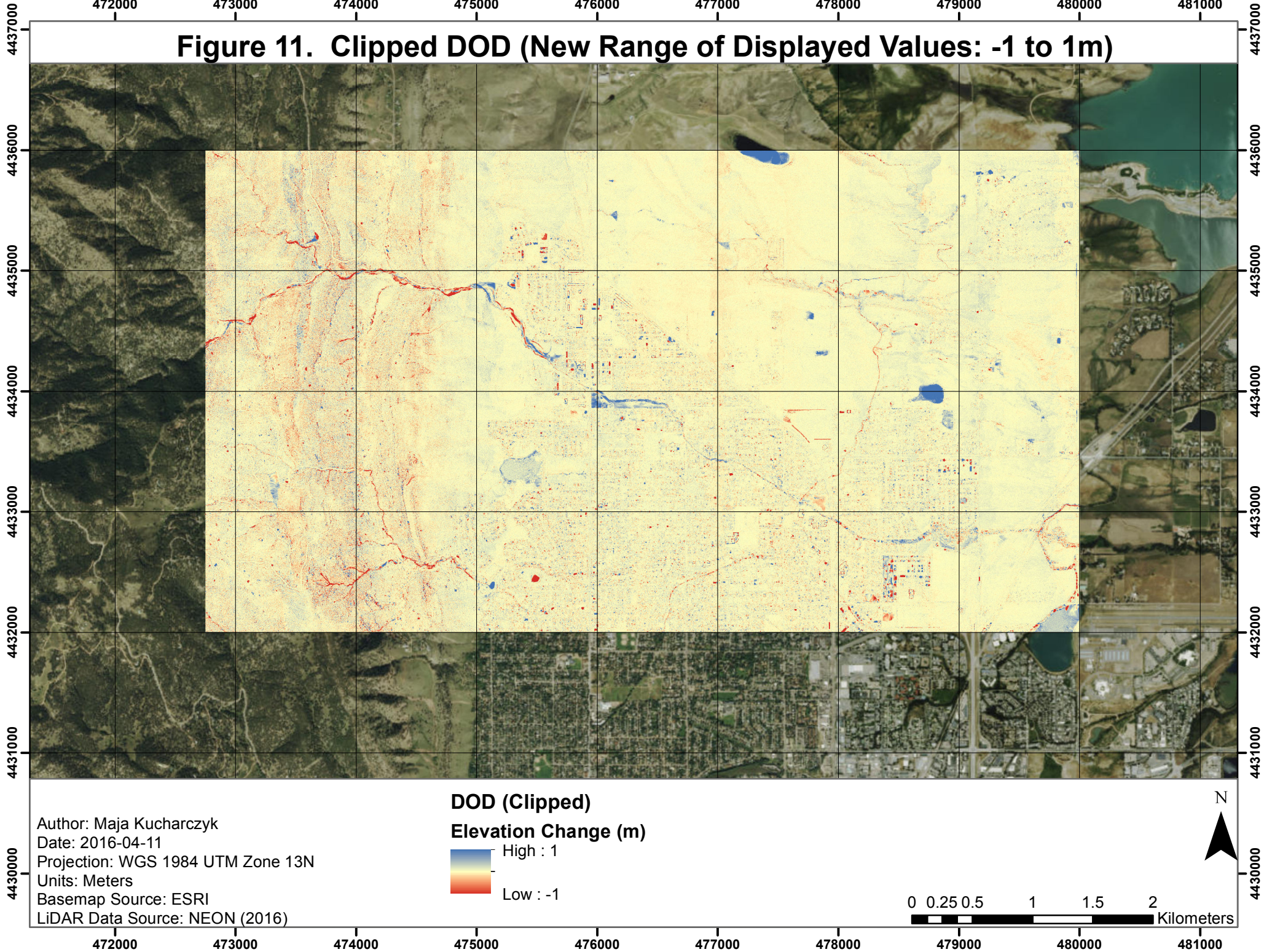
### **3.2.1 Select Areas of Erosion and Deposition**

The selected stream channel is shown in Figure 12. A major area of erosion along the stream channel was bounded by the red polygon. A major area of deposition along the stream channel was bounded by the blue polygon.

### **3.2.2 Calculate Erosion and Deposition Volume Along a Stream Channel**

The volume polygons and output rasters are shown in Figure 13. For the erosion polygon, the total eroded volume was 10,774 cubic meters ( $m^3$ ), while the total deposited volume was 980  $m^3$ . For the deposition polygon, the total eroded volume was 808  $m^3$ , while the total deposited volume was 10,215  $m^3$ .

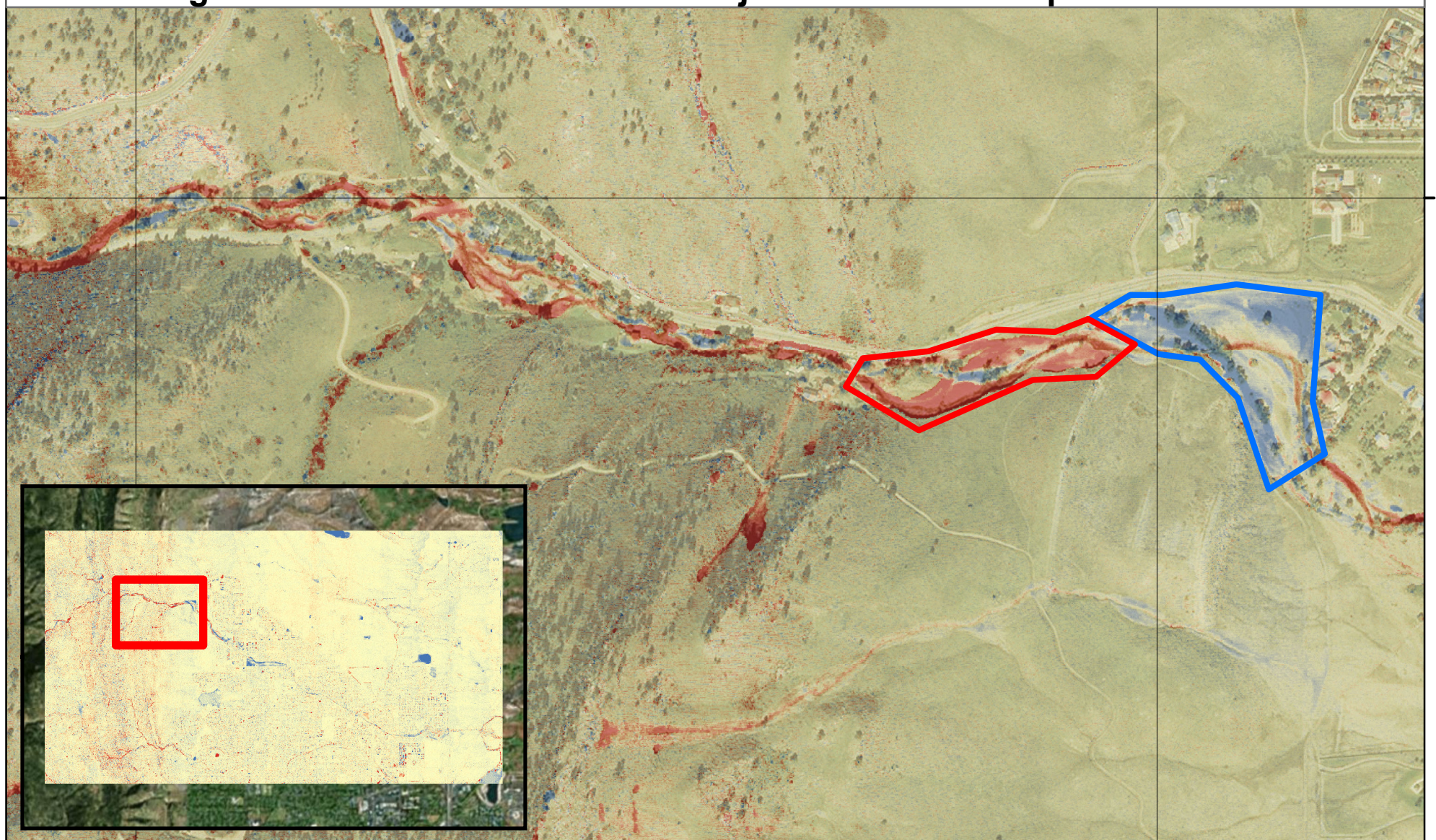
**Figure 11. Clipped DOD (New Range of Displayed Values: -1 to 1m)**



474000

475000

**Figure 12. Stream Channel with Major Erosion and Deposition Areas**



Author: Maja Kucharczyk

Date: 2016-04-11

Projection: WGS 1984 UTM Zone 13N

Units: Meters

Basemap Source: ESRI

LiDAR Data Source: NEON (2016)

**DOD (Clipped)**

**Elevation Change (m)**

High : 1

Low : -1

Erosion Volume Polygon

Deposition Volume Polygon

N

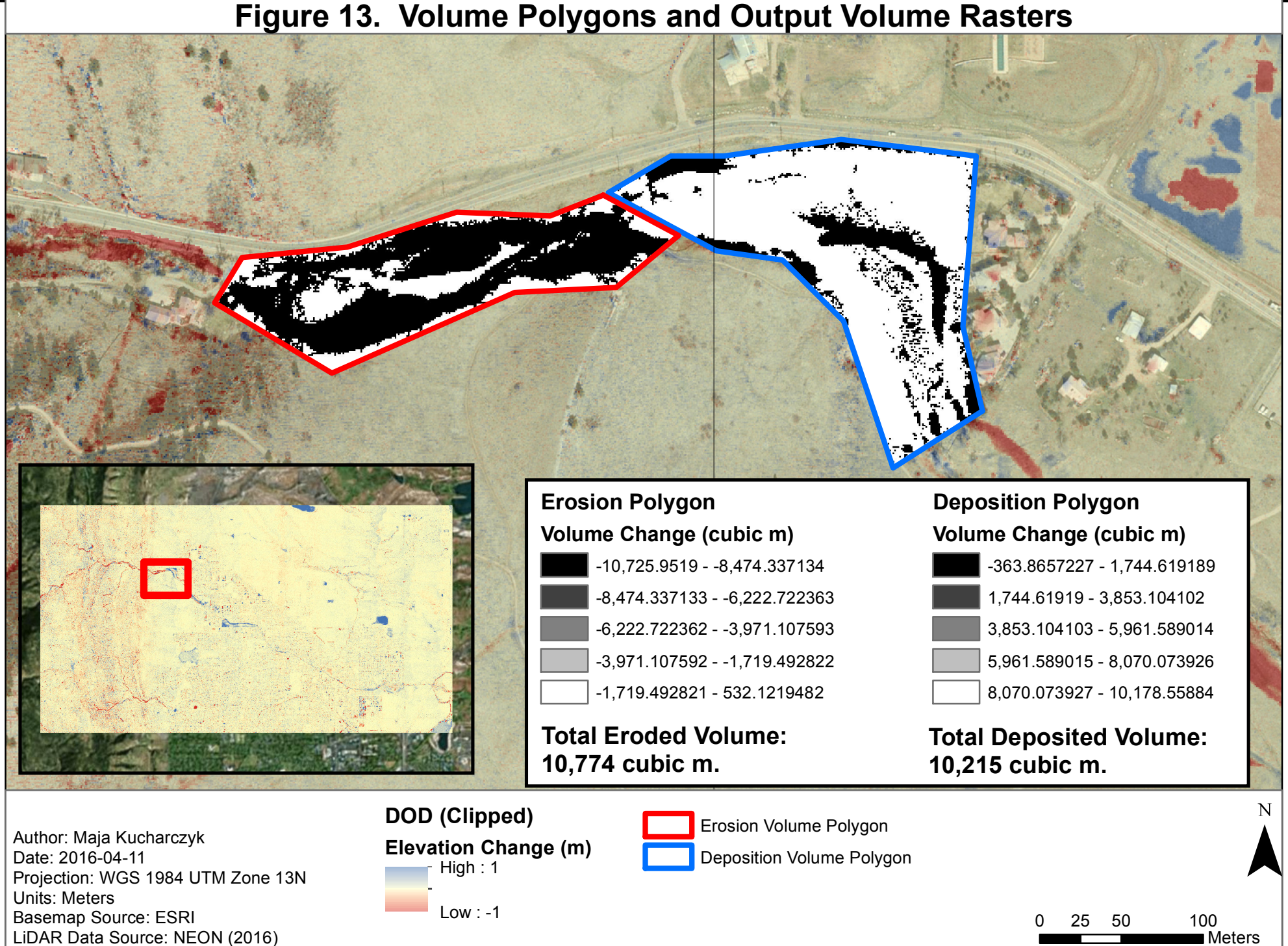


0 50 100 200  
Meters

474000

475000

**Figure 13. Volume Polygons and Output Volume Rasters**



**3.3 Objective 3:** Use the post-flood DTM to determine the slope aspects of the satellite imagery-derived debris flows locations by Morgan, Fitzgerald, & Morgan (2014) and compare the results to those obtained by Coe et al. (2014)

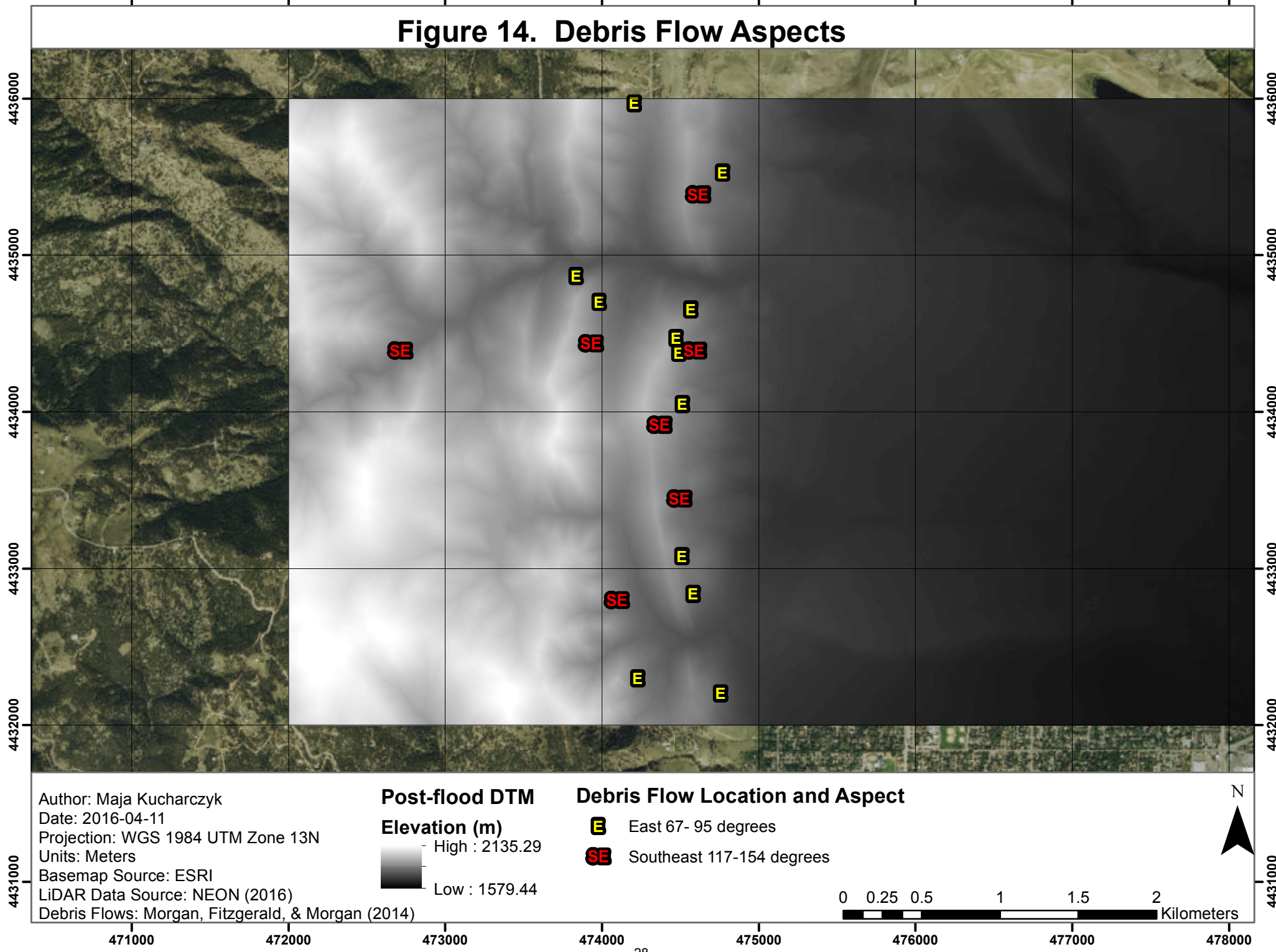
### 3.3.1 Calculate the Aspect of the Possible Debris Flow Locations

Figure 14 shows the 19 debris flow locations within the post-flood DTM. Table 3 summarizes the aspects of the debris flows. Twelve out of nineteen debris flows have aspects in the east direction, and seven out of nineteen debris flows have aspects in the southeast direction. Coe et al. (2014) reported 78 percent (%) of the 1,138 debris flows they surveyed in the Boulder and greater Boulder region initiated on south-facing slopes. The aspects of the debris flows mapped by Morgan, Fitzgerald, & Morgan (2014) within the post-flood DTM were primarily on east and southeast slopes, which makes sense given the movement of floodwater east down the Rocky Mountains.

Table 3. Debris flow aspects.

Debris Flow Location	Aspect (degrees counterclockwise from north)	Aspect Classification
1	66.57	East
2	80.05	
3	84.92	
4	85.94	
5	86.99	
6	87.27	
7	89.17	
8	89.35	
9	92.46	
10	94.24	
11	94.75	
12	95.14	
13	117.38	Southeast
14	119.32	
15	124.42	
16	125.19	
17	132.42	
18	148.69	
19	154.03	

## Figure 14. Debris Flow Aspects



### **3.6 Limitations**

Temporal change detection studies face challenges regarding their inability to conclusively determine that a detected change is attributed to the phenomenon being studied. For this project, any elevation change detected cannot be assumed to be caused by the flood. There are numerous sources for elevation changes to appear on the DOD.

Sensor and post-processing errors can be disguised as physical elevation change. As was shown in Figure 8, points can be incorrectly classified during the LiDAR point cloud processing stage. Also, the pre-and post-flood LiDAR data acquisitions occurred two months before and one month after the flood, respectively. It is not possible to distinguish natural processes from flood processes when viewing topographic change. Also, during the time between the flood occurring and the post-flood LiDAR data acquisition, some of the damage may have been repaired and thus the true extent of the flood damage has not been depicted.

## **4. Conclusion**

The Boulder, Colorado flood of September 2013 resulted in fatalities and billions of dollars in damage. The environmental impacts of the flood have been surveyed and recorded. Using LiDAR data collected over Boulder before and after the flood, topographic change detection has been performed by differencing the elevation datasets. Erosional and depositional volume along stream channels was calculated, and slope aspect of possible debris flow locations was determined. These methods can be applied for damage remediation, in terms of prioritizing areas that have undergone the most topographic change.

## 5. References

- American Society for Photogrammetry and Remote Sensing (ASPRS), 2010. LAS Specification, Version 1.3 – R11. American Society of Photogrammetry & Remote Sensing, 5410 Grosvenor Lane, Suite 210, Bethesda Maryland.
- Coe, J.A., Kean, J.W., Godt, J.W., Baum, R.L., Jones, E.S., Gochis, D.J., & Anderson, G.S. (2014). New insights into debris-flow hazards from an extraordinary event in the Colorado Front Range. *GSA Today*, 24(10), 4-10.
- ESRI. (2016). How Aspect Works. Retrieved from <http://desktop.arcgis.com/en/arcmap/10.3/tools/spatial-analyst-toolbox/how-aspect-works.htm>
- Gochis, D., Schumacher, R., Friedrich, K., Doesken, N., Kelsch, M., Sun, J.,..., & Brown, B. (2015). The Goulden, T., & Kampe, T.U. (2014). NEON AOP Surveys of Boulder Pre and Post 2013 Flood Event. *National Ecological Observatory Network*, Technical Memo 006. Retrieved from [http://www.neoninc.org/sites/default/files/biblio-files/NEON\\_Technical\\_Memo\\_006a\\_BLDR%20Flood\\_Pre\\_Post\\_Assessment.pdf](http://www.neoninc.org/sites/default/files/biblio-files/NEON_Technical_Memo_006a_BLDR%20Flood_Pre_Post_Assessment.pdf)
- Great Colorado Flood of September 2013. *American Meteorological Society*, 1461-1488.
- Morgan, M.L., Fitzgerald, F.S., & Morgan, K.S. (2013). *Preliminary Survey of Debris Flow, Landslide, and Rockfall Deposits as a result of the September 11-14, 2013 Flooding Events, Boulder County, Colorado*. Retrieved from <http://www.arcgis.com/home/item.html?id=39e6c721635f40c8add90112c9d1a646>
- National Ecological Observatory Network (NEON). (2016). *Airborne Data: Boulder Pre-Flood and Post-Flood 2013 Discrete Return LiDAR*. Retrieved from: <http://www.neonscience.org/data-resources/get-data/airborne-data>
- RapidLasso. (2016). LASTools. Retrieved from: <http://rapidlasso.com/lastools/>

## Appendix A

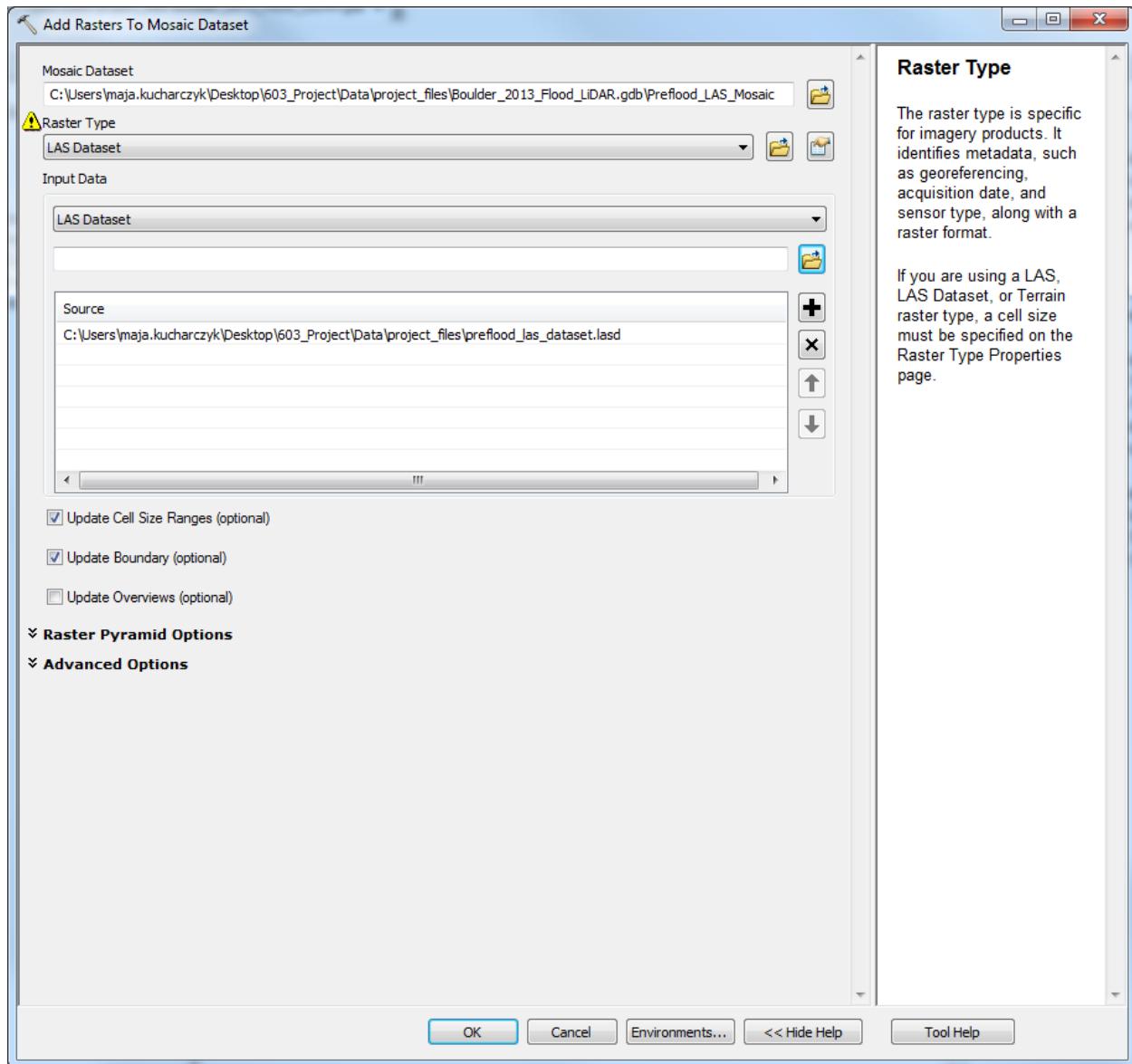


Figure A.1. Add Rasters To Mosaic Dataset tool being used to add the pre-flood LAS Dataset to the pre-flood Mosaic Dataset.

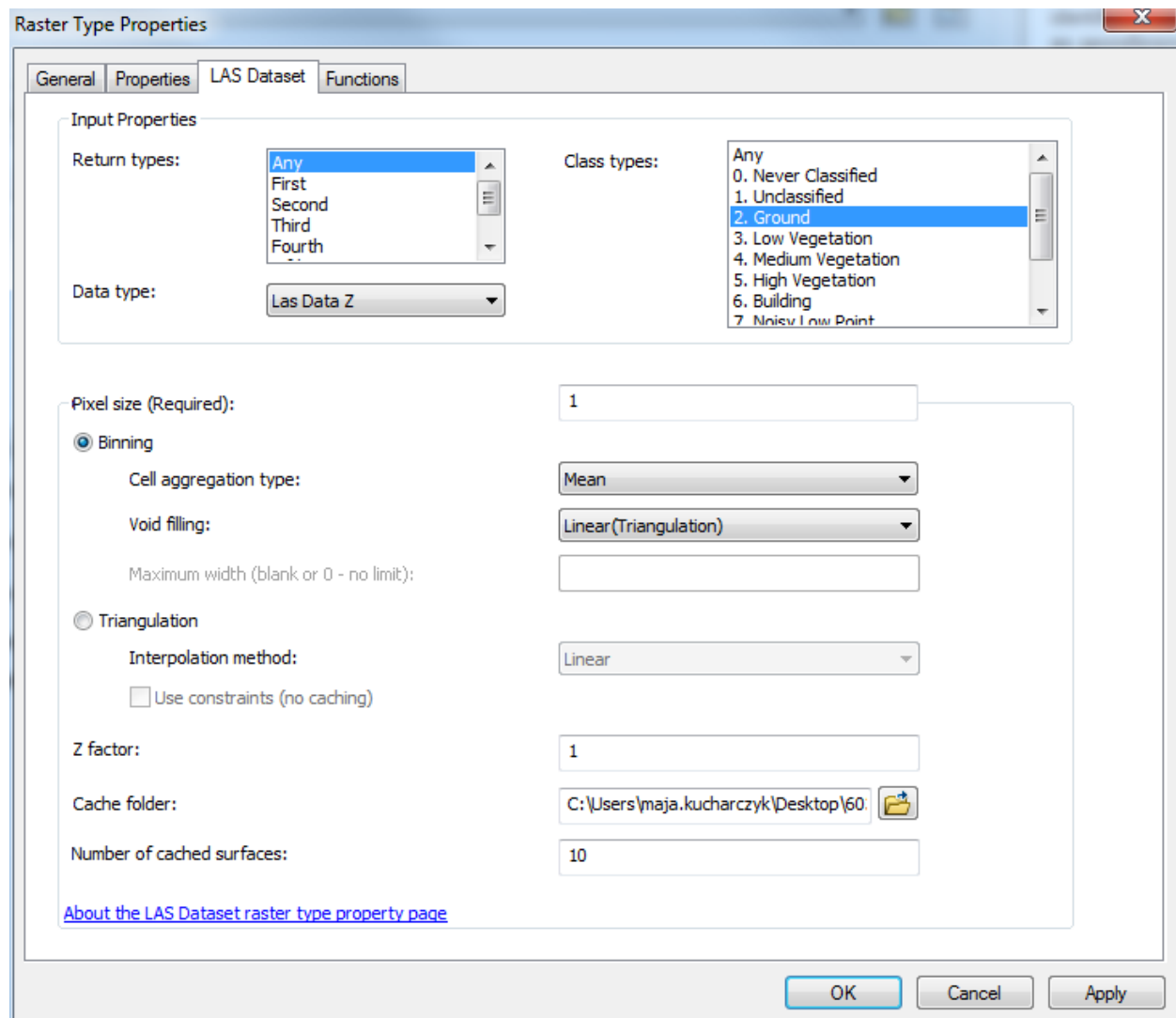


Figure A.2. Raster Type Properties being used to specify the output pre-flood DTM parameters.

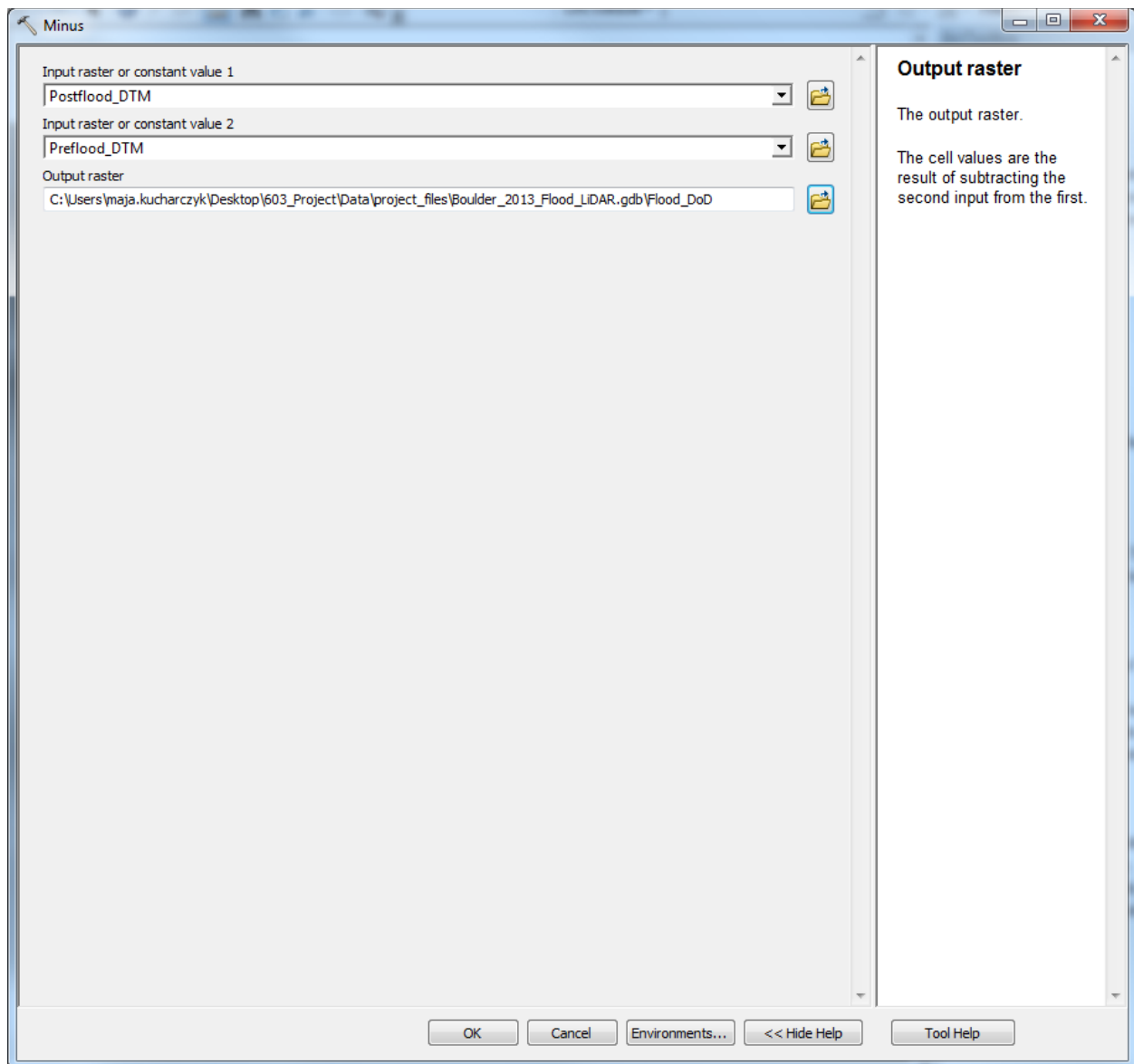


Figure A.3. Minus tool being used to subtract the pre-flood DTM from the post-flood DTM in order to output a DOD.